applied sciences

MDPI

Article

Finite-Time Path Following Control of an Underactuated Marine Surface Vessel with Input and Output Constraints

Mingyu Fu * and Lulu Wang *

College of Intelligent Systems Science and Engineering, Harbin Engineering University, Harbin 150001, China
* Correspondence: fumingyu@hrbeu.edu.cn (M.F.); heuwanglulu@163.com (L.W.)

Received: 20 August 2020; Accepted: 14 September 2020; Published: 16 September 2020

Abstract: This paper develops a finite-time path following control scheme for an underactuated marine surface vessel (MSV) with external disturbances, model parametric uncertainties, position constraint and input saturation. Initially, based on the time-varying barrier Lyapunov function (BLF), the finite-time line-of-sight (FT-LOS) guidance law is proposed to obtain the desired yaw angle and simultaneously constrain the position error of the underactuated MSV. Furthermore, the finite-time path following constraint controllers are designed to achieve tracking control in finite time. Additionally, considering the model parametric uncertainties and external disturbances, the finite-time disturbance observers are proposed to estimate the compound disturbance. For the sake of avoiding the input saturation and satisfying the requirements of finite-time convergence, the finite-time input saturation compensators were designed. The stability analysis shows that the proposed finite-time path following control scheme can strictly guarantee the constraint requirements of the position, and all error signals of the whole control system can converge into a small neighborhood around zero in finite time. Finally, comparative simulation results show the effectiveness and superiority of the proposed finite-time path following control scheme.

Keywords: underactuated marine surface vessel; path following; finite-time; position constraint; input saturation; disturbance observer

1. Introduction

The marine surface vessel (MSV) mainly relies on the guidance system to perform the required control scheme, such as path following, target tracking and path tracking, in which the influences of wind, currents and waves on the ship, which are simply considered in [1–4]. The path following control aims to control the ship to reach and track a predetermined parameterized curve at a certain velocity without time constraints [5]. In the last few years, the control problem of path following for the underactuated MSV has attracted extensive attention in the control field [6–8].

The guidance law is an important component of the path following problem, which aims to compute the desired heading angle for the subsequent controller design by processing path information. The classical guidance laws consist of the line-of-sight (LOS) guidance, constant bearing guidance, and pure pursuit guidance [9]. Especially, because the LOS guidance law has simple and intuitive characteristics, it has been widely used in the path following control of MSV. At an early stage, the classical LOS guidance law for reducing the cross-track error was presented in [10]. However, although the classical LOS guidance laws are simple and effective, they have limitations for the vessel, subject to external disturbances. Then, the integral line-of-sight (ILOS) guidance law was developed by introducing the integral actions into the LOS guidance law, which can eliminate the drifting effect [11,12]. Due to the complexity of the environment and the requirement of the operation accuracy, it is necessary to not only consider the tracking performance of the desired path, but also to ensure that the position errors of the ship during navigation does not have large jitter, otherwise it is not conducive to the accurate path tracking of the ship. In addition, in order to navigate safely, the actuator saturation of the underactuated MSV should be limited. Otherwise, the control performance of the system will deteriorate and lead to the instability of the control system [13]. For the problem of position error constraint and actuator saturation, in [14], a path-following controller based on the error-constrained line-of-sight (EC-LOS) guidance law was presented for an MSV. An asymmetric time-varying barrier Lyapunov function (BLF) and a smooth hyperbolic tangent function were proposed for a fully actuated MSV to address the asymmetrical input and output constraint in [15]. In the case of actuator saturation and external disturbance, a path following control scheme for a MSV with a prescribed performance was presented in [16]. In [17], a control scheme was presented for the underactuated MSV, which considers not only the position error constraint, input saturation, external disturbance and model uncertainties, but also time-varying sideslip. However, the convergence time of the above literature is asymptotically convergent, which implies that exact convergence cannot be guaranteed in finite time, and the influence of the convergence time is not considered. In order to obtain a high-performance solution, this paper proposes an FT-LOS guidance law, which can ensure that the position errors will not exceed the error constraint, and converge into a small neighborhood around zero in finite time.

In addition to the requirements of the error constraints and input saturation, it is also important to consider the effect of convergence time on system performance. The finite-time controller makes the system errors converge in finite time, thereby obtaining faster convergence rate and better disturbance rejection properties. The research on the finite-time control of the underactuated MSV focuses on trajectory tracking control problem. In [18], a finite-time disturbance observer was presented to reduce the environment disturbances, which has the advantages of fast convergence speed and strong robustness. In order to precisely estimate completely external disturbances and unknown dynamics, a finite-time tracking controller was presented for trajectory tracking in [19]. In addition, it improves the robustness and tracking accuracy of the control system. A finite-time sliding mode controller for an USV with model parametric uncertainties and external disturbances was presented in [20]. A path following controller based on a finite-time observer was proposed in [21], which only considers the large sideslip angle and external disturbances. However, the influence of position error constraints on vessel path following control are not considered. In [22], a fuzzy finite-time controller was proposed for the underactuated MSV, subject to external disturbances, parametric uncertainties, sideslip angle and actuator saturation in finite-time, but the position error constraint was not considered in the controller design. Therefore, considering the influence of position error constraint on path following controller, an FT-LOS guidance law was designed by introducing time-varying BLF into the design process of LOS guidance law.

Based on the above observations, this paper presents a finite-time path following control scheme for the underactuated MSV under the conditions of position constraint, external disturbances, model parameter uncertainties, and actuator saturation. The main contributions and superiority of this paper are summarized as follows:

(1) A finite-time line-of-sight (FT-LOS) guidance law is designed by integrating a time-varying BLF into the classical LOS guidance law design process. The proposed FT-LOS guidance law can ensure that the position errors will not exceed the error constraints, and converge into a small neighborhood around zero in finite time.
(2) The finite-time attitude constraint controller and the finite-time velocity constraint controller are designed to achieve tracking control in finite time. A command filter is designed to eliminate the complex calculation of the virtual control law.
(3) The finite-time disturbance observers are proposed to reduce the compound disturbance. In addition the finite-time input saturation compensators are designed to avoid the actuator saturation and satisfy the finite-time convergence requirement.

(4) The stability analysis shows that the proposed finite-time path following control algorithm can strictly guarantee the constraint requirement of the position, and all error signals of the whole closed-loop control system can converge into a small neighborhood around zero in finite time. Comparative simulation results illustrate the effectiveness and superiority of the proposed finite-time control scheme.

The rest of this paper is arranged as follows. Section 2 presents the preliminaries and problem formulation. The finite-time path following control algorithm is proposed in Section 3, consisting of the FT-LOS guidance law design, the finite-time attitude constraint controller design, and the finite-time velocity constraint controller design. Section 4 analyses the stability of the whole closed-loop control system. Comparative simulation results are shown and analyzed in Section 5 to demonstrate the effectiveness and superiority of the proposed finite-time path following control algorithm. Finally, the conclusions are shown in Section 6.

2. Preliminaries and Problem Formulation

2.1. Preliminaries

Notation 1. *In this paper,* $|\cdot|$ *stands for the absolute value of a scalar;* $\overset{\wedge}{(\cdot)}$ *stands for the estimate of* $(\cdot)$*;* $\overset{\sim}{(\cdot)} = \overset{\wedge}{(\cdot)} - (\cdot)$ *defines the estimation error.*

Definition 1. *([23]) A barrier Lyapunov function is a scalar function* $V(x)$ *defined with respect to the system* $\dot{x} = f(x)$ *on an open region D containing the origin. The* $V(x)$ *is continuous, is positive definite, has continuous first-order partial derivatives at every point of D, has the property* $V(x) \to \infty$ *as x approaches the boundary of D, and satisfies* $V(x) \leq b, \forall t \geq 0$ *along the solution of* $\dot{x} = f(x)$ *for* $x(0) \in D$ *and some positive constant b.*

Definition 2. *([24]) Consider the following system:*

$$\dot{x}(t) = f(x(t)) \tag{1}$$

where $f : D \to \mathbb{R}^n$ *is continuous on an open neighborhood* $D \subseteq \mathbb{R}^n$ *of the origin and* $f(0) = 0$*. The origin is said to be a finite-time-stable equilibrium of (1) if there exists an open neighborhood* $N \subseteq D$ *of the origin and a function* $T : N\backslash\{0\} \to (0, \infty)$*, called the settling-time function, such that the following statements hold:*

(i) Finite-time convergence: For every $x(0) \in N\backslash\{0\}$*,* $x(t)$ *is defined on* $[0, T(x))$*,* $x(t) \in N\backslash\{0\}$ *for all* $t \in [0, T(x))$*, and* $\lim_{t \to T(x)} x(t) = 0$*.*

(ii) Lyapunov stability: For every open neighborhood U_ε *of 0 there exists an open subset* U_δ *of N containing 0 such that, for every* $x(0) \in U_\delta\backslash 0$*,* $x(t) \in U_\varepsilon$ *for all* $t \in [0, T(x))$*.*

The origin is said to be a globally finite-time-stable equilibrium if it is a finite-time-stable equilibrium with $D = N = \mathbb{R}^n$*.*

Lemma 1. *([25]) Suppose that there is a positive definite continuous Lyapunov function* $V(x, t)$ *defined on* $U_1 \subset \mathbb{R}^n$ *of the origin, and*

$$\dot{V}(x, t) \leq -c_1 V^\alpha(x, t) - c_2 V(x, t), \forall x \in U_1\backslash\{0\} \tag{2}$$

where $c_1 > 0$*,* $c_2 > 0$ *and* $0 < \alpha < 1$*. Then the origin of system (1) is locally finite-time stable and the settling time can be given by* $T \leq \ln(1+(c_2/c_1)V^{1-\alpha}(x_0, t_0))/(c_2 - c_2\alpha)$*.*

Lemma 2. *([26]) For any $x_i \in \mathbb{R}$, $i = 1, 2, ..., n$, and a real number $0 < p \leq 1$, then*

$$\left(\sum_{i=1}^{n} |x_i|\right)^p \leq \sum_{i=1}^{n} |x_i|^p \tag{3}$$

2.2. Model of Underactuated Marine Surface Vessel

The dynamics and kinematics equations for the underactuated MSV are defined by [9]. The kinematics model of the underactuated MSV can be written as follows:

$$\begin{cases} \dot{x} = u\cos(\psi) - v\sin(\psi) \\ \dot{y} = u\sin(\psi) + v\cos(\psi) \\ \dot{\psi} = r \end{cases} \tag{4}$$

where $[x, y, \psi]^T$ represents the surge position, the sway position and the heading angle of the MSV in the earth-fixed inertial frame; $[u, v, r]^T$ represents the surge velocity, the sway velocity, and the yaw rate of the MSV in the body-fixed frame.

In order to simplify the dynamics model, it is necessary to make reasonable assumption as follows:

Assumption 1. [21]

(1). The heave, pitch and roll motions are neglected in path following on the horizontal plane.
(2). The vehicle is rigid body and its mass distribution is homogeneous, and the vehicle is port/starboard symmetric.
(3). The origin of body-fixed is located at the center of gravity of the vehicle.

The dynamics model of the underactuated MSV can be written as follows:

$$\begin{cases} m_{11}\dot{u} = \underbrace{m_{22}vr - d_{11}u}_{f_u} + \tau_{wu} + \tau_u \\ m_{22}\dot{v} = -\underbrace{m_{11}ur - d_{22}v}_{f_v} + \tau_{wv} \\ m_{33}\dot{r} = \underbrace{(m_{11} - m_{22})uv - d_{33}r}_{f_r} + \tau_{wr} + \tau_r \end{cases} \tag{5}$$

where the positive constant terms m_{11}, m_{22}, m_{33} represent the vessel inertia including added mass. The positive constant terms d_{11}, d_{22}, d_{33} represent the hydrodynamic damping, which can be obtained by using system identification. Therefore, $f_j (j = u, v, r)$ have the model parametric uncertainties. $\tau_{wj} (j = u, v, r)$ are the time-varying environment disturbances. The surge force τ_u and the yaw moment τ_r are the control inputs. In practical engineering, because of the physical constraints of the vessel's actuators, the control force and moment can be expressed as follows:

$$\tau_i = \begin{cases} \tau_{i\max}, \textit{if } \tau_{ic} > \tau_{i\max} \\ \tau_{ic}, \quad \textit{if } \tau_{i\min} \leq \tau_{ic} \leq \tau_{i\max} \\ \tau_{i\min}, \textit{if } \tau_{ic} < \tau_{i\min} \end{cases}, i = u, r \tag{6}$$

Assumption 2. *The compound disturbances $d_j = \tau_{wj} + f_j (j = u, v, r)$ and their respective derivatives are bounded, which satisfy the following inequalities: $|d_j| \leq \bar{d}_j$, $|\dot{d}_j| \leq C_{d_j}$, where $\bar{d}_j$ and C_{d_j} are positive constants.*

2.3. Path Following Error Dynamic

In order to converge to the desired path, a general and effective guidance law for the path following control problem is a look-ahead LOS guidance law. Figure 1 shows the geometrical illustration of the LOS guidance law for the MSV.

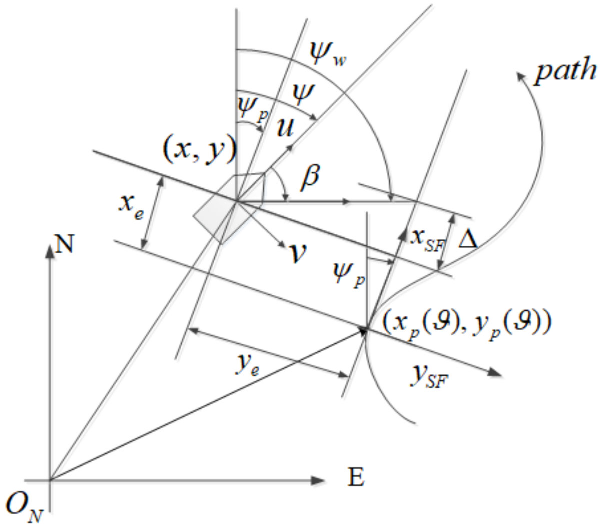

Figure 1. The geometrical illustration of LOS guidance for a MSV.

The desired path is defined as $X_p(\vartheta) = \left[x_p(\vartheta), y_p(\vartheta)\right]^T$, where ϑ represents the path variable. The path tangent angle is calculated by

$$\psi_p(\vartheta) = \text{arctan2}(y'_p(\vartheta), x'_p(\vartheta)) \tag{7}$$

where $x'_p = \frac{\partial x_p}{\partial \vartheta}$ and $y'_p = \frac{\partial y_p}{\partial \vartheta}$. The along-track error x_e and the cross-track error y_e can be written as follows:

$$\begin{bmatrix} x_e \\ y_e \end{bmatrix} = \begin{bmatrix} \cos\psi_p & \sin\psi_p \\ -\sin\psi_p & \cos\psi_p \end{bmatrix} \begin{bmatrix} x - x_p \\ y - y_p \end{bmatrix} \tag{8}$$

The differentiation of x_e can be obtained:

$$\begin{aligned} \dot{x}_e = &\dot{x}\cos\psi_p + \dot{y}\sin\psi_p - \dot{x}_p\cos\psi_p - \dot{y}_p\sin\psi_p \\ &+ \dot{\psi}_p \underbrace{\left(-(x - x_p)\sin\psi_p + (y - y_p)\cos\psi_p\right)}_{\text{cross-track error } y_e} \end{aligned} \tag{9}$$

Then, substituting (4) into (9) yields

$$\begin{aligned} \dot{x}_e &= u\cos(\psi - \psi_p) - v\sin(\psi - \psi_p) + \dot{\psi}_p y_e - \dot{\vartheta}\sqrt{{x'_p}^2 + {y'_p}^2} \\ &= U\cos(\psi - \psi_p + \beta) + \dot{\psi}_p y_e - \dot{\vartheta}\sqrt{{x'_p}^2 + {y'_p}^2} \end{aligned} \tag{10}$$

where $U = \sqrt{u^2 + v^2}$ denotes the speed of the vessel and $\beta = \text{arctan2}(v, u)$ is the vessel's sideslip angle.

Similarly, the differentiation of y_e can be obtained:

$$\begin{aligned} \dot{y}_e = &-\dot{x}\sin\psi_p + \dot{y}\cos\psi_p + \dot{x}_p\sin\psi_p - \dot{y}_p\cos\psi_p \\ &- \dot{\psi}_p \underbrace{\left((x - x_p)\cos\psi_p + (y - y_p)\sin\psi_p\right)}_{\text{along-track error } x_e} \end{aligned} \tag{11}$$

and substituting (4) into (11) results in,

$$\begin{aligned} \dot{y}_e &= u\sin(\psi - \psi_p) + v\cos(\psi - \psi_p) - \dot{\psi}_p x_e \\ &= U\sin(\psi - \psi_p + \beta) - \dot{\psi}_p x_e \end{aligned} \tag{12}$$

Finally, similar to [27], the derivatives of errors become

$$\begin{cases} \dot{x}_e = U\cos(\psi - \psi_p + \beta) + \dot{\psi}_p y_e - \dot{\vartheta}\sqrt{x_p'^2 + y_p'^2} \\ \dot{y}_e = U\sin(\psi - \psi_p + \beta) - \dot{\psi}_p x_e \end{cases} \tag{13}$$

Considering the mathematical model of an underactuated MSV with the external disturbances, model parametric uncertainties, position constraint and input saturation, the control objectives of this paper are as follows: (1) Design the FT-LOS guidance law to ensure that the position error will not exceed the error constraint, and converge into a small neighborhood around zero in finite time. (2) The finite-time attitude constraint controller τ_r and the finite-time velocity constraint controller τ_u are designed to make the underactuated MSV track the desired path at the desired speed in finite time. In addition, it has faster convergence speed and better disturbance rejection performance. (3) All error signals of the whole closed-loop control system can converge into a small neighborhood around zero in finite time, and position errors meet the constraint requirements, that is to say, $|x_e| < k_x(t)$, $|y_e| < k_y(t)$, where $\{k_x(t), k_y(t)\}$ are differentiable time-varying error constrains.

To facilitate the controller design, we make the assumption as follows:

Assumption 3. *The initial position errors satisfy the prescribed constraints* $|x_e(t_0)| < k_x(t_0)$, $|y_e(t_0)| < k_y(t_0)$.

3. Finite-Time Path Following Control Algorithm Design

In this section, the finite-time path following control scheme is proposed to realize the control objectives. The finite-time path following control scheme for the underactuated MSV includes three parts: (1) FT-LOS guidance law design; (2) the finite-time attitude constraint controller design; (3) the finite-time velocity constraint controller design. The schematic diagram of the whole close-loop control system is shown in Figure 2. The specific design process of the finite-time path following control algorithm will be introduced in the following subsections.

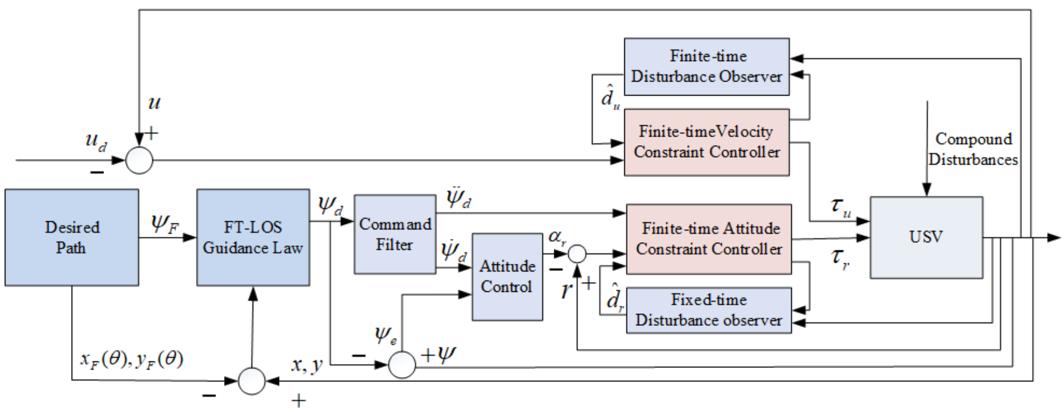

Figure 2. The block diagram of path following control.

3.1. Ft-Los Guidance Law Design

The FT-LOS guidance law is proposed to obtain the update law and the desired heading angle.

The time-varying BLF will be integrated into the FT-LOS guidance to ensure the position error constraints. Define the time-varying BLF as follows:

$$\begin{aligned} V_1 &= \frac{1}{2}\log\frac{k_x^2(t)}{k_x^2(t) - x_e^2} + \frac{1}{2}\log\frac{k_y^2(t)}{k_y^2(t) - y_e^2} \\ &= \frac{1}{2}\log\frac{1}{1-\xi_x^2} + \frac{1}{2}\log\frac{1}{1-\xi_y^2} \end{aligned} \tag{14}$$

where $\xi_x = \frac{x_e}{k_x(t)}$ and $\xi_y = \frac{y_e}{k_y(t)}$.

Taking the derivative of V_1, we obtain

$$\dot{V}_1 = \frac{\xi_x}{1-\xi_x^2}\left(\frac{\dot{x}_e}{k_x(t)} - \frac{x_e\dot{k}_x(t)}{k_x^2(t)}\right) + \frac{\xi_y}{1-\xi_y^2}\left(\frac{\dot{y}_e}{k_y(t)} - \frac{y_e\dot{k}_y(t)}{k_y^2(t)}\right) \tag{15}$$

Substituting (13) into (15), we obtain

$$\begin{aligned}\dot{V}_1 = & \frac{x_e}{k_x^2(t)-x_e^2}\left(U\cos(\psi-\psi_p+\beta) - \dot{\vartheta}\sqrt{{x'_p}^2+{y'_p}^2} - \frac{x_e\dot{k}_x(t)}{k_x(t)}\right) \\ & - \frac{y_e^2}{k_y^2(t)-y_e^2}\frac{\dot{k}_y(t)}{k_y(t)} + \frac{y_e}{k_y^2(t)-y_e^2}U\sin(\psi-\psi_p+\beta) \\ & + \frac{x_e}{k_x^2(t)-x_e^2}\dot{\psi}_p y_e\left(1-\frac{k_x^2(t)-x_e^2}{k_y^2(t)-y_e^2}\right)\end{aligned} \tag{16}$$

Taking the time derivative of ψ_p yields

$$\dot{\psi}_p = \dot{\vartheta}\frac{y''_p x'_p - x''_p y'_p}{{x'_p}^2+{y'_p}^2} \tag{17}$$

Invoking (17) into (16), we have

$$\begin{aligned}\dot{V}_1 = & \frac{x_e}{k_x^2(t)-x_e^2}\left(U\cos(\psi-\psi_p+\beta) - \dot{\vartheta}\sigma\right) \\ & - \frac{x_e^2}{k_x^2(t)-x_e^2}\frac{\dot{k}_x(t)}{k_x(t)} - \frac{y_e^2}{k_y^2(t)-y_e^2}\frac{\dot{k}_y(t)}{k_y(t)} \\ & + \frac{y_e}{k_y^2(t)-y_e^2}U\sin(\psi-\psi_p+\beta)\end{aligned} \tag{18}$$

with $\sigma = \sqrt{{x'_p}^2+{y'_p}^2} - y_e\frac{y''_p x'_p - x''_p y'_p}{{x'_p}^2+{y'_p}^2}\left(1-\frac{k_x^2(t)-x_e^2}{k_y^2(t)-y_e^2}\right)$.

The update law and the desired heading angle are designed as

$$\dot{\vartheta} = \frac{U\cos(\psi-\psi_p+\beta)+\delta_x}{\sigma} \tag{19}$$

$$\psi_d = \psi_p - \beta - \arctan(\delta_y, \Delta) \tag{20}$$

$$\delta_x = \frac{k_1}{x_e}\log\frac{k_x^2(t)}{k_x^2(t)-x_e^2} + \frac{k_2}{x_e}\log^{\frac{3}{4}}\left(\frac{k_x^2(t)}{k_x^2(t)-x_e^2}\right) - \frac{x_e\dot{k}_x(t)}{k_x(t)} \tag{21}$$

$$\delta_y = \frac{k_3}{y_e}\log\frac{k_y^2(t)}{k_y^2(t)-y_e^2} + \frac{k_4}{y_e}\log^{\frac{3}{4}}\left(\frac{k_y^2(t)}{k_y^2(t)-y_e^2}\right) - \frac{y_e}{U}\frac{\dot{k}_y(t)}{k_y(t)}\sqrt{\delta_y^2+\Delta^2} \tag{22}$$

where k_1, k_2, k_3 and k_4 are positive design parameters; $0 < \Delta_{\min} \leq \Delta \leq \Delta_{\max}$ denotes the look-ahead distance; To avoid $\sigma = 0$, we can take $\sigma = \sigma_0\mathrm{sgn}(\sigma)$ when $|\sigma| < \sigma_0$, where σ_0 is a small positive parameter.

Substituting (19)–(22) into (18) results in

$$\begin{aligned}
\dot{V}_1 &= -\frac{x_e}{k_x^2(t)-x_e^2}\delta_x - \frac{x_e^2}{k_x^2(t)-x_e^2}\frac{\dot{k}_x(t)}{k_x(t)} - \frac{y_e^2}{k_y^2(t)-y_e^2}\frac{\dot{k}_y(t)}{k_y(t)} - \frac{y_e U}{k_y^2(t)-y_e^2}\frac{\delta_y}{\sqrt{\delta_y^2+\Delta^2}} + \frac{y_e U \phi_1 \psi_e}{k_y^2(t)-y_e^2} \\
&= -\frac{k_1}{k_x^2(t)-x_e^2}\log\frac{k_x^2(t)}{k_x^2(t)-x_e^2} - \frac{k_3 U}{(k_y^2(t)-y_e^2)\sqrt{\delta_y^2+\Delta^2}}\log\frac{k_y^2(t)}{k_y^2(t)-y_e^2} \\
&\quad - \frac{k_2}{k_x^2(t)-x_e^2}\log^{\frac{3}{4}}\left(\frac{k_x^2(t)}{k_x^2(t)-x_e^2}\right) - \frac{k_4 U}{(k_y^2(t)-y_e^2)\sqrt{\delta_y^2+\Delta^2}}\log^{\frac{3}{4}}\left(\frac{k_y^2(t)}{k_y^2(t)-y_e^2}\right) \\
&\quad + \frac{y_e U \phi_1 \psi_e}{k_y^2(t)-y_e^2}
\end{aligned} \tag{23}$$

where

$$\phi_1 = \frac{(1-\cos\psi_e)}{\psi_e}\frac{\delta_y}{\sqrt{\delta_y^2+\Delta^2}} + \frac{\sin\psi_e}{\psi_e}\frac{\Delta}{\sqrt{\delta_y^2+\Delta^2}} \tag{24}$$

and $\psi_e = \psi - \psi_d$.

Remark 1. *In (24), we have* $\left|\frac{1-\cos\psi_e}{\psi_e}\right| < 0.73$, $\left|\frac{\sin\psi_e}{\psi_e}\right| \leq 1$, $\left|\frac{\Delta}{\sqrt{\delta_y^2+\Delta^2}}\right| \leq 1$ *and* $\left|\frac{\delta_y}{\sqrt{\delta_y^2+\Delta^2}}\right| \leq 1$. *Therefore,* $\phi_1 \leq 1.73$ *is bounded.*

3.2. The Finite-Time Attitude Constraint Controller Design

Step 1. (Kinematics controller). Define the yaw tracking error as follows:

$$\psi_e = \psi - \psi_d \tag{25}$$

Define the Lyapunov function V_2 as follows:

$$V_2 = \frac{1}{2}\psi_e^2 \tag{26}$$

Taking the time derivative of V_2, we obtain

$$\dot{V}_2 = \psi_e\,(r - \dot{\psi}_d) \tag{27}$$

Step 2. (Dynamics controller). Define the yaw angle rate error as follows:

$$r_e = r - \alpha_r \tag{28}$$

where α_r is the virtual control law.

Substituting (28) into (27) yields

$$\dot{V}_2 = \psi_e\,(r_e + \alpha_r - \dot{\psi}_d) \tag{29}$$

In order to avoid the complicated calculation of the derivative of α_r, the proposed command filter is shown in Figure 3. Furthermore, an auxiliary system is presented to compensate for the estimation error.

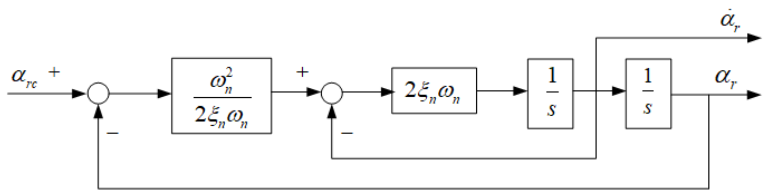

Figure 3. Configuration of the command filter.

A second-order command filter is expressed as follows:

$$\begin{cases} \dot{\rho}_1 = \rho_2 \\ \dot{\rho}_2 = -2\xi_n\omega_n \left(\rho_2 + \dfrac{\omega_n^2}{2\xi_n\omega_n}(\rho_1 - \alpha_{rc}) \right) \end{cases} \tag{30}$$

where ξ_n and ω_n are positive design parameters; α_{rc} is the input signal of the second-order command filter; ρ_1 and ρ_2 denote the estimations of α_r and $\dot{\alpha}_r$, respectively.

Define the estimation error as follow:

$$\Delta\alpha_r = \alpha_r - \alpha_{rc} \tag{31}$$

Substituting (31) into (29) yields

$$\dot{V}_2 = \psi_e \left(r_e + \alpha_{rc} + \Delta\alpha_r - \dot{\psi}_d \right) \tag{32}$$

Therefore, design a nominal virtual yaw rate α_{rc} for (32) as follows:

$$\alpha_{rc} = -k_\psi \psi_e - k_{\psi 1} |\psi_e|^{\frac{1}{2}} + \dot{\psi}_d + c_r \zeta_r - \frac{c_r^2}{2}\psi_e - \frac{y_e U \phi_1}{k_y^2 - y_e^2} \tag{33}$$

where k_ψ, $k_{\psi 1}$ and c_r denote the positive design constants. To compensate the estimation error $\Delta\alpha_r$ of the virtual yaw rate, the auxiliary system is presented as follows:

$$\dot{\zeta}_r = \begin{cases} 0, & |\zeta_r| \le \zeta_r^* \\ -a_r\zeta_r - a_{r1}|\zeta_r|^{\frac{1}{2}} + b_r\Delta\alpha_r - \left(\frac{1}{2} b_r^2 \Delta\alpha_r^2 + \psi_e \Delta\alpha_r \right) \zeta_r^{-1}, & |\zeta_r| > \zeta_r^* \end{cases} \tag{34}$$

where $a_r > 1$, $a_{r1} > 0$ and $b_r > 0$; ζ_r^* is a positive parameter.

The Lyapunov function is defined as follows:

$$V_3 = V_2 + \frac{1}{2}\zeta_r^2 \tag{35}$$

Invoking (33) and (34), the time derivative of V_3 is given by

$$\begin{aligned} \dot{V}_3 =& \dot{V}_2 + \zeta_r \dot{\zeta}_r \\ =& \psi_e r_e - k_\psi \psi_e^2 - k_{\psi 1} |\psi_e|^{\frac{3}{2}} + c_r \psi_e \zeta_r - \frac{1}{2} c_r^2 \psi_e^2 - a_r \zeta_r^2 - a_{r1} |\zeta_r|^{\frac{3}{2}} \\ &+ b_r \zeta_r \Delta\alpha_r - \frac{1}{2} b_r^2 \Delta{\alpha_r}^2 - \frac{y_e U \phi_1 \psi_e}{k_y^2 - y_e^2} \end{aligned} \tag{36}$$

Based on the Young's inequality, we can obtain

$$c_r \psi_e \zeta_r \le \frac{1}{2} c_r^2 \psi_e^2 + \frac{1}{2} \zeta_r^2 \tag{37}$$

$$b_r\zeta_r\Delta\alpha_r \leq \frac{1}{2}b_r^2\Delta\alpha_r^2 + \frac{1}{2}\zeta_r^2 \tag{38}$$

Substituting (37) and (38) into (36), we have

$$\begin{aligned}\dot{V}_3 \leq & -k_\psi\psi_e^2 - k_{\psi1}|\psi_e|^{\frac{3}{2}} - (a_r-1)\zeta_r^2 - a_{r1}\,|\zeta_r|^{\frac{3}{2}} \\ & + \psi_e r_e - \frac{y_e U\phi_1\psi_e}{k_y^2 - y_e^2}\end{aligned} \tag{39}$$

Taking the time derivative of r_e along (5), we have

$$\dot{r}_e = \dot{r} - \dot{\alpha}_r = \frac{1}{m_{33}}\left(\tau_r + d_r\right) - \dot{\alpha}_r \tag{40}$$

The Lyapunov function is defined as follows:

$$V_4 = V_3 + \frac{1}{2}m_{33}r_e^2 \tag{41}$$

Taking the time derivative of V_4 along (39) and (40), we have

$$\begin{aligned}\dot{V}_4 \leq & -k_\psi\psi_e^2 - k_{\psi1}|\psi_e|^{\frac{3}{2}} - (a_r-1)\zeta_r^2 - a_{r1}\,|\zeta_r|^{\frac{3}{2}} + \psi_e r_e \\ & - \frac{y_e U\phi_1\psi_e}{k_y^2 - y_e^2} + r_e\left(\tau_r + d_r - m_{33}\dot{\alpha}_r\right)\end{aligned} \tag{42}$$

Next, a finite-time disturbance observer is designed in order to estimate the compound disturbance d_r:

$$\begin{cases}\dot{\hat{r}} = \dfrac{1}{m_{33}}\left[\tau_r - b_1\tilde{r} - b_2|\tilde{r}|^{\gamma_1}\operatorname{sgn}(\tilde{r}) - \bar{d}_r\operatorname{sgn}(\tilde{r})\right] \\ \hat{d}_r = m_{33}\dot{\hat{r}} - \tau_r = -b_1\tilde{r} - b_2|\tilde{r}|^{\gamma_1}\operatorname{sgn}(\tilde{r}) - \bar{d}_r\operatorname{sgn}(\tilde{r})\end{cases} \tag{43}$$

where $\hat{d}_r$ is the observation value of the disturbance, $0 < \gamma_1 < 1$, b_1, b_2 are positive design constants and define the estimation error as $\tilde{r} = \hat{r} - r$. Then, taking the time derivative of $\tilde{r}$ results in

$$\dot{\tilde{r}} = \frac{1}{m_{33}}\left[-b_1\tilde{r} - b_2|\tilde{r}|^{\gamma_1}\operatorname{sgn}(\tilde{r}) - \bar{d}_r\operatorname{sgn}(\tilde{r}) - d_r\right] \tag{44}$$

Theorem 1. *For the mathematical model of an underactuated MSV (4) and (5), considering the compound disturbance d_r, a finite-time disturbance observer is designed as (43), then the disturbance observation error $\tilde{d}_r$ can converge to 0 in finite time.*

Proof. Consider a Lyapunov function as follows:

$$V_{d_r} = \frac{1}{2}\tilde{r}^2 \tag{45}$$

Taking the time derivative of V_{d_r} results in

$$\begin{aligned}\dot{V}_{d_r} &= \tilde{r}\frac{1}{m_{33}}\left[-b_1\tilde{r} - b_2|\tilde{r}|^{\gamma_1}\operatorname{sgn}(\tilde{r}) - \bar{d}_r\operatorname{sgn}(\tilde{r}) - d_r\right] \\ &\leq -b_1\frac{1}{m_{33}}\tilde{r}^2 - b_2\frac{1}{m_{33}}|\tilde{r}|^{\gamma_1+1} \\ &= -2\frac{b_1}{m_{33}}V_{d_r} - 2^{(\gamma_1+1)/2}\frac{b_2}{m_{33}}V_{d_r}^{(\gamma_1+1)/2} \\ &= -\chi_1 V_{d_r} - \chi_2 V_{d_r}^{(\gamma_1+1)/2}\end{aligned} \tag{46}$$

where $\chi_1 = 2\frac{b_1}{m_{33}}$ and $\chi_2 = 2^{(\gamma_1+1)/2}\frac{b_2}{m_{33}}$. According to the Lemma 1, the estimation error $\tilde{r}$ converges to 0 in finite time, and the convergence time is: $T_1 \leq \frac{\ln\left(1+\frac{\chi_1}{\chi_2}V_{d_r}^{1-(\gamma_1+1)/2}\right)}{\chi_1(1-(\gamma_1+1)/2)}$.

The observation error of the compound disturbance d_r is

$$\begin{aligned}\tilde{d}_r &= \hat{d}_r - d_r = m_{33}\dot{\hat{r}} - \tau_r - (m_{33}\dot{r} - \tau_r) \\ &= m_{33}\dot{\tilde{r}}\end{aligned} \tag{47}$$

Because it is proven that the estimation error $\tilde{r}$ converges to zero in finite time, the disturbance observation error $\tilde{d}_r$ can converge to 0 in finite time, that is $\tilde{d}_r = 0$, $\forall t \geq T_1$. The Theorem 1 has been proven. □

To handle the actuator saturation (6), a finite-time attitude input saturation compensator is designed as follows:

$$\dot{\chi}_r = -k_{\chi_{r1}}\chi_r - k_{\chi_{r2}}S_{\chi_r} + \Delta\tau_r \tag{48}$$

where χ_r is the output of the finite-time attitude input saturation compensator, $k_{\chi_{r1}} > 0$, $k_{\chi_{r2}} > 0$, $\Delta\tau_r = \tau_r - \tau_{rc}$. S_{χ_r} is designed as follows:

$$S_{\chi_r} = \begin{cases} |\chi_r|^{\frac{1}{2}}\,\mathrm{sgn}(\chi_r), & \text{if } |\chi_r| \geq \varepsilon_{\chi_r} \\ \frac{3}{2}\varepsilon_{\chi_r}^{-\frac{1}{2}}\chi_r - \frac{1}{2}\varepsilon_{\chi_r}^{-\frac{3}{2}}\chi_r^2, & \text{else} \end{cases} \tag{49}$$

The finite-time attitude tracking constraint controller can be designed as follows:

$$\tau_{rc} = m_{33}\dot{\alpha}_r - k_r r_e - k_{r1}|r_e|^{\frac{1}{2}} - \psi_e - \hat{d}_r + k_{\chi_r}\chi_r \tag{50}$$

where k_r, k_{r1} and k_{χ_r} are positive parameters.

The Lyapunov function is defined as follows:

$$V_r = V_4 + \frac{1}{2}\chi_r^2 \tag{51}$$

Taking the time derivative of V_r along (48)–(50), we have

$$\begin{aligned}\dot{V}_r \leq &- k_\psi\psi_e^2 - k_{\psi1}|\psi_e|^{\frac{3}{2}} - (a_r-1)\zeta_r^2 - a_{r1}|\zeta_r|^{\frac{3}{2}} \\ &- \frac{y_e U\phi_1\psi_e}{k_y^2 - y_e^2} - k_r r_e^2 - k_{r1}|r_e|^{\frac{3}{2}} - r_e\tilde{d}_r + k_{\chi_r}\chi_r r_e \\ &+ r_e\Delta\tau_r - k_{\chi_{r1}}\chi_r^2 - k_{\chi_{r2}}|\chi_r|^{\frac{3}{2}} + \chi_r\Delta\tau_r\end{aligned} \tag{52}$$

According to the Theorem 1, for $\forall t \geq T_1$, the disturbance observation error $\tilde{d}_r = 0$. Therefore, for $\forall t \geq T_1$, there are

$$\begin{aligned}\dot{V}_r \leq &- k_\psi\psi_e^2 - k_{\psi1}|\psi_e|^{\frac{3}{2}} - (a_r-1)\zeta_r^2 - a_{r1}|\zeta_r|^{\frac{3}{2}} \\ &- \frac{y_e U\phi_1\psi_e}{k_y^2 - y_e^2} - k_r r_e^2 - k_{r1}|r_e|^{\frac{3}{2}} + k_{\chi_r}\chi_r r_e \\ &+ r_e\Delta\tau_r - k_{\chi_{r1}}\chi_r^2 - k_{\chi_{r2}}|\chi_r|^{\frac{3}{2}} + \chi_r\Delta\tau_r\end{aligned} \tag{53}$$

Based on the Young's inequality, we can obtain

$$r_e\chi_r \leq \frac{1}{2}r_e^2 + \frac{1}{2}\chi_r^2 \tag{54}$$

$$r_e\Delta\tau_r \leq \frac{1}{2}r_e^2 + \frac{1}{2}\Delta\tau_r^2 \tag{55}$$

$$\chi_r \Delta\tau_r \leq \frac{1}{2}\chi_r^2 + \frac{1}{2}\Delta\tau_r^2 \tag{56}$$

Substituting (54)–(56) into (53), we have

$$\begin{aligned} \dot{V}_r \leq & -k_\psi \psi_e^2 - k_{\psi 1}|\psi_e|^{\frac{3}{2}} - (a_r - 1)\zeta_r^2 - a_{r1}|\zeta_r|^{\frac{3}{2}} \\ & - \frac{y_e U \phi_1 \psi_e}{k_y^2 - y_e^2} - \left(k_r - \frac{k_{\chi_r}}{2} - \frac{1}{2}\right) r_e^2 - k_{r1}|r_e|^{\frac{3}{2}} \\ & - \left(k_{\chi_{r1}} - \frac{k_{\chi_r}}{2} - \frac{1}{2}\right)\chi_r^2 - k_{\chi_{r2}}|\chi_r|^{\frac{3}{2}} + \Delta\tau_r^2 \end{aligned} \tag{57}$$

3.3. The Finite-Time Velocity Constraint Controller Design

Define the surge velocity tracking error as follows:

$$u_e = u - u_d \tag{58}$$

where u_d is the desired surge velocity.

Consider a Lyapunov function as follows:

$$V_5 = \frac{1}{2} m_{11} u_e^2 \tag{59}$$

Taking the time derivative of V_5 along (5) and (58), we have

$$\dot{V}_5 = u_e(d_u + \tau_u - m_{11}\dot{u}_d) \tag{60}$$

Next, a finite-time disturbance observer is designed to estimate the compound disturbance d_u:

$$\begin{cases} \dot{\hat{u}} = \dfrac{1}{m_{11}}\left[\tau_u - b_3\tilde{u} - b_4|\tilde{u}|^{\gamma_2}\operatorname{sgn}(\tilde{u}) - \bar{d}_u \operatorname{sgn}(\tilde{u})\right] \\ \hat{d}_u = m_{11}\dot{\hat{u}} - \tau_u = -b_3\tilde{u} - b_4|\tilde{u}|^{\gamma_2}\operatorname{sgn}(\tilde{u}) - \bar{d}_u \operatorname{sgn}(\tilde{u}) \end{cases} \tag{61}$$

where $\hat{d}_u$ is the observation value of the disturbance, $0 < \gamma_2 < 1$, b_3, b_4 are positive design constants and define the estimation error as $\tilde{u} = \hat{u} - u$. Then, taking the time derivative of $\tilde{u}$ results in

$$\dot{\tilde{u}} = \frac{1}{m_{11}}\left[-b_3\tilde{u} - b_4|\tilde{u}|^{\gamma_2}\operatorname{sgn}(\tilde{u}) - \bar{d}_u \operatorname{sgn}(\tilde{u}) - d_u\right] \tag{62}$$

Theorem 2. *For the mathematical model of an underactuated MSV (4) and (5), considering the compound disturbance d_u, a finite-time disturbance observer is designed as (61), then the disturbance observation error $\tilde{d}_u$ can converge to 0 in finite time.*

Proof. Define the Lyapunov function as follows:

$$V_{d_u} = \frac{1}{2}\tilde{u}^2 \tag{63}$$

Taking the time derivative of V_{d_u} results in

$$\begin{aligned}\dot{V}_{d_u} &= \tilde{u}\frac{1}{m_{11}}\left[-b_3\tilde{u} - b_4|\tilde{u}|^{\gamma_2}\operatorname{sgn}(\tilde{u}) - \bar{d}_u\operatorname{sgn}(\tilde{u}) - d_u\right] \\ &\leq -b_3\frac{1}{m_{11}}\tilde{u}^2 - b_4\frac{1}{m_{11}}|\tilde{u}|^{\gamma_2+1} \\ &= -2\frac{b_3}{m_{11}}V_{d_u} - 2^{(\gamma_2+1)/2}\frac{b_4}{m_{11}}V_{d_u}^{(\gamma_2+1)/2} \\ &= -\chi_3 V_{d_u} - \chi_4 V_{d_u}^{(\gamma_2+1)/2}\end{aligned} \tag{64}$$

where $\chi_3 = 2\frac{b_3}{m_{11}}$ and $\chi_4 = 2^{(\gamma_2+1)/2}\frac{b_4}{m_{11}}$. According to the Lemma 1, the estimation error $\tilde{u}$ converges to 0 in finite time, and the convergence time is: $T_2 \leq \frac{\ln\left(1+\frac{\chi_3}{\chi_4}V_{d_u}^{1-(\gamma_2+1)/2}\right)}{\chi_3(1-(\gamma_2+1)/2)}$.

The observation error of the compound disturbance d_u is

$$\begin{aligned}\tilde{d}_u &= \hat{d}_u - d_u = m_{11}\dot{\hat{u}} - \tau_u - (m_{11}\dot{u} - \tau_u) \\ &= m_{11}\dot{\tilde{u}}\end{aligned} \tag{65}$$

Because it is proven that the estimation error $\tilde{u}$ converges to zero in finite time, the disturbance observation error $\tilde{d}_u$ converges to 0 in finite time, that is $\tilde{d}_u = 0$, $\forall t \geq T_2$. Theorem 2 has been proven. □

To handle the actuator saturation (6), a finite-time velocity input saturation compensator is designed as follows:

$$\dot{\chi}_u = -k_{\chi_{u1}}\chi_u - k_{\chi_{u2}}S_{\chi_u} + \Delta\tau_u \tag{66}$$

where χ_u is the output of the finite-time velocity input saturation compensator, $k_{\chi_{u1}} > 0$, $k_{\chi_{u2}} > 0$, $\Delta\tau_u = \tau_u - \tau_{uc}$. S_{χ_u} is designed as follows:

$$S_{\chi_u} = \begin{cases} |\chi_u|^{\frac{1}{2}}\operatorname{sgn}(\chi_u), & \text{if } |\chi_u| \geq \varepsilon_{\chi_u} \\ \frac{3}{2}\varepsilon_{\chi_u}^{-\frac{1}{2}}\chi_u - \frac{1}{2}\varepsilon_{\chi_u}^{-\frac{3}{2}}\chi_u^2, & \text{else}\end{cases} \tag{67}$$

Then, the finite-time surge velocity constraint controller is designed as follows:

$$\tau_{uc} = m_{11}\dot{u}_d - k_u u_e - k_{u1}|u_e|^{\frac{1}{2}} - \hat{d}_u + k_{\chi_u}\chi_u \tag{68}$$

where k_u, k_{u1} and k_{χ_u} are control parameters.

Consider a Lyapunov function as follows:

$$V_u = V_5 + \frac{1}{2}\chi_u^2 \tag{69}$$

Taking the time derivative of V_u along (66)–(68), we have

$$\begin{aligned}\dot{V}_u =& -k_u u_e^2 - k_{u1}|u_e|^{\frac{3}{2}} - u_e\tilde{d}_u + k_{\chi_u}\chi_u u_e \\ &+ u_e\Delta\tau_u - k_{\chi_{u1}}\chi_u^2 - k_{\chi_{u2}}|\chi_u|^{\frac{3}{2}} + \chi_u\Delta\tau_u\end{aligned} \tag{70}$$

According to the Theorem 2, for $\forall t \geq T_2$, the disturbance observation error $\tilde{d}_u = 0$. Therefore, for $\forall t \geq T_2$, there are

$$\begin{aligned}\dot{V}_u =& -k_u u_e^2 - k_{u1}|u_e|^{\frac{3}{2}} + k_{\chi_u}\chi_u u_e \\ &+ u_e\Delta\tau_u - k_{\chi_{u1}}\chi_u^2 - k_{\chi_{u2}}|\chi_u|^{\frac{3}{2}} + \chi_u\Delta\tau_u\end{aligned} \tag{71}$$

Based on the Young's inequality, we can obtain

$$u_e\chi_u \leq \frac{1}{2}u_e^2 + \frac{1}{2}\chi_u^2 \tag{72}$$

$$u_e\Delta\tau_u \leq \frac{1}{2}u_e^2 + \frac{1}{2}\Delta\tau_u^2 \tag{73}$$

$$\chi_u\Delta\tau_u \leq \frac{1}{2}\chi_u^2 + \frac{1}{2}\Delta\tau_u^2 \tag{74}$$

Substituting (72)–(74) into (71), we have

$$\begin{aligned} \dot{V}_u \leq &-\left(k_u - \frac{k_{\chi_u}}{2} - \frac{1}{2}\right)u_e^2 - k_{u1}|u_e|^{\frac{3}{2}} \\ &-\left(k_{\chi_{u1}} - \frac{k_{\chi_u}}{2} - \frac{1}{2}\right)\chi_u^2 - k_{\chi_{u2}}|\chi_u|^{\frac{3}{2}} + \Delta\tau_u^2 \end{aligned} \tag{75}$$

4. Stability Analysis

Theorem 3. *Consider the whole control system of the mathematical model (4) and (5) with external disturbances, model parametric uncertainties, and input saturation, and suppose that Assumptions 1 and 2 are satisfied. The update law and the desired heading angle are presented as (19) and (20), the auxiliary system is developed as (34), the finite-time disturbance observers are designed as (43) and (61), the finite-time tracking constraint controllers are designed as (50) and (68), and the finite-time input saturation compensators are designed as (48) and (66). Select the appropriate controller parameters: $k_r > \frac{k_{\chi r}}{2} + \frac{1}{2}$, $k_{\chi_{r1}} > \frac{k_{\chi r}}{2} + \frac{1}{2}$, $k_u > \frac{k_{\chi u}}{2} + \frac{1}{2}$ and $k_{\chi_{u1}} > \frac{k_{\chi u}}{2} + \frac{1}{2}$, then the following conclusions are valid:*

(i) *All the error signals of the whole control system are uniformly ultimately bounded. Additionally, position errors meet the constraint requirements, that is $|x_e| < k_x(t)$ and $|y_e| < k_y(t)$.*
(ii) *The tracking error of an underactuated MSV can converge into a small neighborhood around zero in finite time.*

Proof. Construct the Lyapunov function of the whole control system as follows:

$$\begin{aligned} V =& V_1 + V_r + V_u \\ =& \frac{1}{2}\log\frac{k_x^2}{k_x^2 - x_e^2} + \frac{1}{2}\log\frac{k_y^2}{k_y^2 - y_e^2} + \frac{1}{2}\psi_e^2 + \frac{1}{2}\zeta_r^2 \\ &+ \frac{1}{2}m_{33}r_e^2 + \frac{1}{2}\chi_r^2 + \frac{1}{2}m_{11}u_e^2 + \frac{1}{2}\chi_u^2 \end{aligned} \tag{76}$$

By virtue of (23), (57), (75) and Lemma 2, the differentiation of V can be obtained:

$$\begin{aligned} \dot{V} \leq &-\frac{k_1}{k_x^2 - x_e^2}\log\frac{k_x^2}{k_x^2 - x_e^2} - \frac{k_3 U}{(k_y^2 - y_e^2)\sqrt{\delta_y^2 + \Delta^2}}\log\frac{k_y^2}{k_y^2 - y_e^2} \\ &-\frac{k_2}{k_x^2 - x_e^2}\log^{\frac{3}{4}}\left(\frac{k_x^2}{k_x^2 - x_e^2}\right) - \frac{k_4 U}{(k_y^2 - y_e^2)\sqrt{\delta_y^2 + \Delta^2}}\log^{\frac{3}{4}}\left(\frac{k_y^2}{k_y^2 - y_e^2}\right) \\ &- k_\psi\psi_e^2 - k_{\psi 1}|\psi_e|^{\frac{3}{2}} - (a_r - 1)\zeta_r^2 - a_{r1}|\zeta_r|^{\frac{3}{2}} - (k_r - \frac{k_{\chi_r}}{2} - \frac{1}{2})r_e^2 \\ &- k_{r1}|r_e|^{\frac{3}{2}} - (k_{\chi_{r1}} - \frac{k_{\chi_r}}{2} - \frac{1}{2})\chi_r^2 - k_{\chi_{r2}}|\chi_r|^{\frac{3}{2}} - (k_u - \frac{k_{\chi_u}}{2} - \frac{1}{2})u_e^2 \\ &- k_{u1}|u_e|^{\frac{3}{2}} - (k_{\chi_{u1}} - \frac{k_{\chi_u}}{2} - \frac{1}{2})\chi_u^2 - k_{\chi_{u2}}|\chi_u|^{\frac{3}{2}} + \Delta\tau_r^2 + \Delta\tau_u^2 \\ \leq &- K_1 V - K_2 V^{\frac{3}{4}} + K_3 \end{aligned} \tag{77}$$

where $K_1 = \min\left\{\begin{array}{l} \frac{2k_1}{k_x^2 - x_e^2}, \frac{2k_3 U}{(k_y^2 - y_e^2)\sqrt{\delta_y^2 + \Delta^2}}, 2k_\psi, 2(a_r - 1), \frac{2}{m_{33}}(k_r - \frac{k_{\chi_r}}{2} - \frac{1}{2}), \\ 2(k_{\chi_{r1}} - \frac{k_{\chi_r}}{2} - \frac{1}{2}), \frac{2}{m_{11}}(k_u - \frac{k_{\chi_u}}{2} - \frac{1}{2}), 2(k_{\chi_{u1}} - \frac{k_{\chi_u}}{2} - \frac{1}{2}) \end{array}\right\}$, $K_2 = \min\left\{\begin{array}{l} \frac{2^{\frac{3}{4}} k_2}{k_x^2 - x_e^2}, \frac{2^{\frac{3}{4}} k_4 U}{(k_y^2 - y_e^2)\sqrt{\delta_y^2 + \Delta^2}}, 2^{\frac{3}{4}} k_{\psi 1}, 2^{\frac{3}{4}} a_{r1}, \\ \left(\frac{2}{m_{33}}\right)^{\frac{3}{4}} k_{r1}, 2^{\frac{3}{4}} k_{\chi_{r2}}, \left(\frac{2}{m_{11}}\right)^{\frac{3}{4}} k_{u1}, 2^{\frac{3}{4}} k_{\chi_{u2}} \end{array}\right\}$ and $K_3 = \Delta\tau_r^2 + \Delta\tau_u^2$.

(i) According to (77), we have

$$\dot{V} \leq -K_1 V - K_2 V^{\frac{3}{4}} + K_3 \leq -K_1 V + K_3 \tag{78}$$

Because $\frac{2k_1}{k_x^2 - x_e^2} \geq \epsilon$, $\frac{2k_3 U}{(k_y^2 - y_e^2)\sqrt{\delta_y^2 + \Delta^2}} \geq \kappa$, similar to [15] and [20], solving the inequality (78) yields

$$0 \leq V \leq \Gamma = \left(V(0) - \frac{K_3}{K_1}\right) e^{-K_1 t} + \frac{K_3}{K_1} \tag{79}$$

Obviously, the BLF (14) is bounded. Therefore, it can be seen intuitively obtained that x_e, y_e, ψ_e, ζ_r, u_e, r_e, χ_u and χ_r are uniformly ultimately bounded. In addition, the BLF (14) satisfies the following inequalities:

$$\begin{array}{l} \frac{1}{2}\log\frac{k_x^2}{k_x^2 - x_e^2} \leq V \leq \Gamma \\ \frac{1}{2}\log\frac{k_y^2}{k_y^2 - y_e^2} \leq V \leq \Gamma \end{array} \tag{80}$$

Then, by solving [80], we obtain:

$$\begin{array}{l} |x_e| \leq k_x\sqrt{1 - e^{-2\Gamma}} < k_x \\ |y_e| \leq k_y\sqrt{1 - e^{-2\Gamma}} < k_y \end{array} \tag{81}$$

Therefore, this means that the position errors of the underactuated MSV meet the constraint requirements—i.e., $|x_e| < k_x$, $|y_e| < k_y$.

(ii) When $V \geq \frac{K_3}{\Pi K_1}$, $K_3 \leq \Pi K_1 V$, where $0 < \Pi < 1$. Therefore, from (77), we can see:

$$\begin{aligned} \dot{V} &\leq -K_1 V - K_2 V^{\frac{3}{4}} + K_3 \\ &\leq -(1 - \Pi)K_1 V - K_2 V^{\frac{3}{4}} \end{aligned} \tag{82}$$

From Lemma 1, we can infer that V can converge to region $\left\{\Omega : \Omega \leq \frac{K_3}{\Pi K_1}\right\}$ in finite time. The convergence time is: $T = \frac{4}{(1-\Pi)K_1}\ln\frac{(1-\Pi)K_1 V^{\frac{1}{4}}(0) + K_2}{K_2}$. This means that the position tracking errors $|x_e| < k_x$, $|y_e| < k_y$ in T. Similarly, the yaw tracking error ψ_e, the yaw angle rate tracking error r_e, the surge velocity tracking error u_e, and the states χ_u, χ_r of the input saturation compensators converge into a small neighborhood around zero in T. According to Theorems 1 and 2, the observation errors $\tilde{d}_r$, $\tilde{d}_u$ of disturbance observers converge to 0 in T_1 and T_2, respectively. □

5. Simulation

In this section, the effectiveness and superiority of the proposed finite-time control scheme are verified by comparative simulation. The model parameters of the underactuated MSV are given as: $m_{11} = 25.8$, $m_{22} = 33.8$, $m_{33} = 2.76$, $d_{11} = 0.93$, $d_{22} = 2.89$, $d_{33} = 0.5$. The desired path is chosen as $X_p = [50\sin(\vartheta/50), \vartheta]^T$. The initial position is chosen as $X_0 = [2, 2]^T$. The initial surge velocity is chosen as $u_0 = 0.2$, and the desired surge velocity is chosen as $u_d = 1$. The initial value of other states is set as zero. The time-varying external disturbances are simulated as: $\tau_{wu} = 0.1\sin(0.1t) + 0.5\sin(0.05t)$, $\tau_{wv} = 0.05\sin(0.05t)$, $\tau_{wr} = 0.1\sin(0.1t) + 0.1\sin(0.05t)$.

The position error constraints are selected as $k_x(t) = 6e^{-0.15t} + 0.5$, $k_y(t) = 6e^{-0.15t} + 0.5$, and the input saturation limitations are set as $\tau_{u\max} = 4N$, $\tau_{u\min} = -4N$, $\tau_{r\max} = 7N$ and $\tau_{r\min} = -7N$. The control parameters are selected as $k_1 = 0.1$, $k_2 = 2$, $k_3 = 70$, $k_4 = 1$, $\Delta = 10$, $k_\psi = 10$, $k_{\psi 1} = 0.7$, $b_1 = 2$, $b_2 = 1$, $k_{\chi_{r1}} = 1$, $k_{\chi_{r2}} = 1$, $k_{\chi_r} = 0.01$, $k_r = 5$, $k_{r1} = 0.01$, $b_3 = 2$, $b_4 = 1$, $k_{\chi_{u1}} = 1$, $k_{\chi_{u2}} = 0.01$, $k_{\chi_u} = 0.01$, $k_u = 15$, $k_{u1} = 0.02$, $a_r = 2.5$, $a_{r1} = 0.01$, $b_r = 2.5$, $c_r = 2.5$.

To better show the effectiveness and superiority of the proposed finite-time path following control scheme, the comparison is constructed with the EC-LOS guidance law [14] and backstepping controller. The EC-LOS guidance law is given as follows:

$$\begin{cases} \dot{\theta} = \dfrac{U\cos(\psi - \psi_p + \beta) + \theta_s}{\sigma} \\ \psi_d = \psi_p - \beta + \arctan(-\theta_e, \Delta) \end{cases} \tag{83}$$

where $\theta_s = \frac{k_{\varepsilon s}}{\varepsilon_s}\frac{k_{cs}^2}{\pi}\sin\left(\frac{\pi\varepsilon_s^2}{2k_{cs}^2}\right)\cos\left(\frac{\pi\varepsilon_s^2}{2k_{cs}^2}\right) + k_{\varepsilon s0}\varepsilon_s$ and $\theta_e = \frac{k_{\varepsilon e}}{\varepsilon_e}\frac{k_{ce}^2}{\pi}\sin\left(\frac{\pi\varepsilon_e^2}{2k_{ce}^2}\right)\cos\left(\frac{\pi\varepsilon_e^2}{2k_{ce}^2}\right) + k_{\varepsilon e0}\varepsilon_e$. In addition, the EC- LOS controller parameters are given as follows: $k_{\varepsilon s} = 2$, $k_{\varepsilon e} = 2$, $k_{\varepsilon s0} = 0.2$, $k_{\varepsilon e0} = 0.2$, $\Delta = 12$.

The simulation results are described in Figures 4–10. Figure 4 shows the desired path and the actual path of the underactuated MSV under two guidance laws. It is shown that the proposed control scheme can control the vessel to follow the desired path quickly, which converges faster than the control scheme based on the EC-LOS guidance law. Figure 5 illustrates the velocities u, v and r of the underactuated MSV under two guidance laws, in which the vessel can quickly reach the desired surge velocity u_d under the proposed control scheme. Figures 6 and 7 show the along-track error and the cross-track error of the underactuated MSV under two guidance laws. As shown in the Figures 6 and 7, both the along-track error and the cross-track error can quickly converge into a small neighborhood around zero under two guidance laws, and they will not exceed the position error constraints. However, the convergence rate of the along-track error and the cross-track error under the FT-LOS guidance law is faster than that under the EC-LOS guidance law. The comparison between the observation error of the finite-time disturbance observer and that of the disturbance observer is depicted in Figure 8. From Figure 8, we can see that the observation errors $\tilde{d}_u$, $\tilde{d}_r$ of the disturbance observer converge to 0 in about 25 s and 27 s, respectively, and the observation errors $\tilde{d}_u$, $\tilde{d}_r$ of the finite-time disturbance observer converge to 0 in about 15 s and 10 s, respectively, which are shorter than the convergence times of the observation errors of the disturbance observer. The surge force τ_u and the yaw moment τ_r of the underactuated MSV under input saturation are shown in Figures 9 and 10, respectively. Under the finite-time input saturation compensator, the surge force and yaw moment of the underactuated MSV are all within the ranges of the input saturation constraint. Consequently, from the simulation results, it can be concluded that the proposed finite-time path following control scheme is more efficient and provides a better dynamic performance.

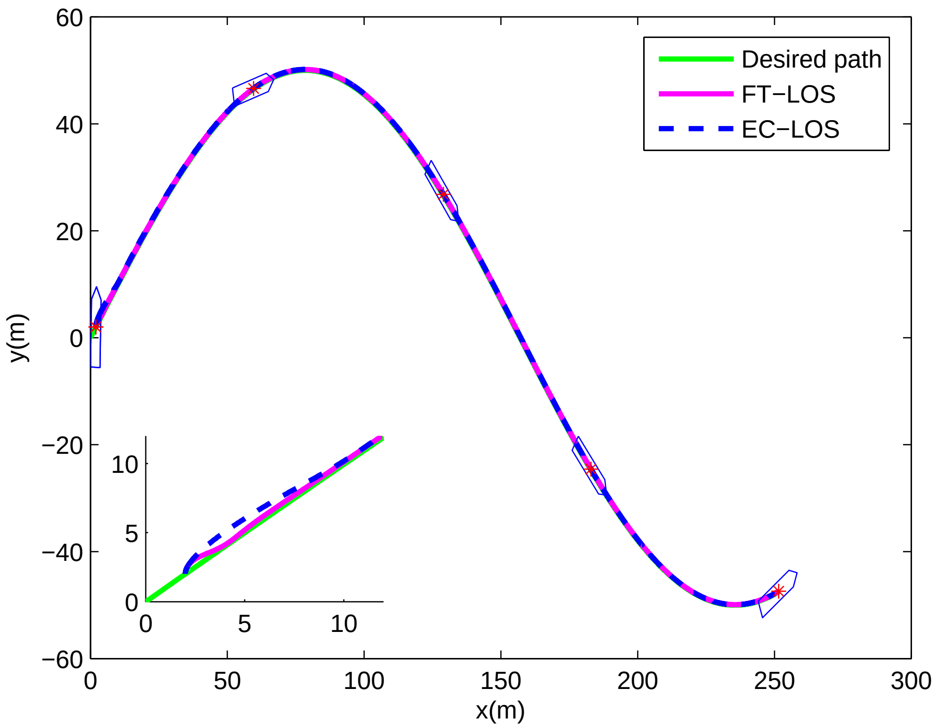

Figure 4. Desired path and actual path of the underactuated MSV.

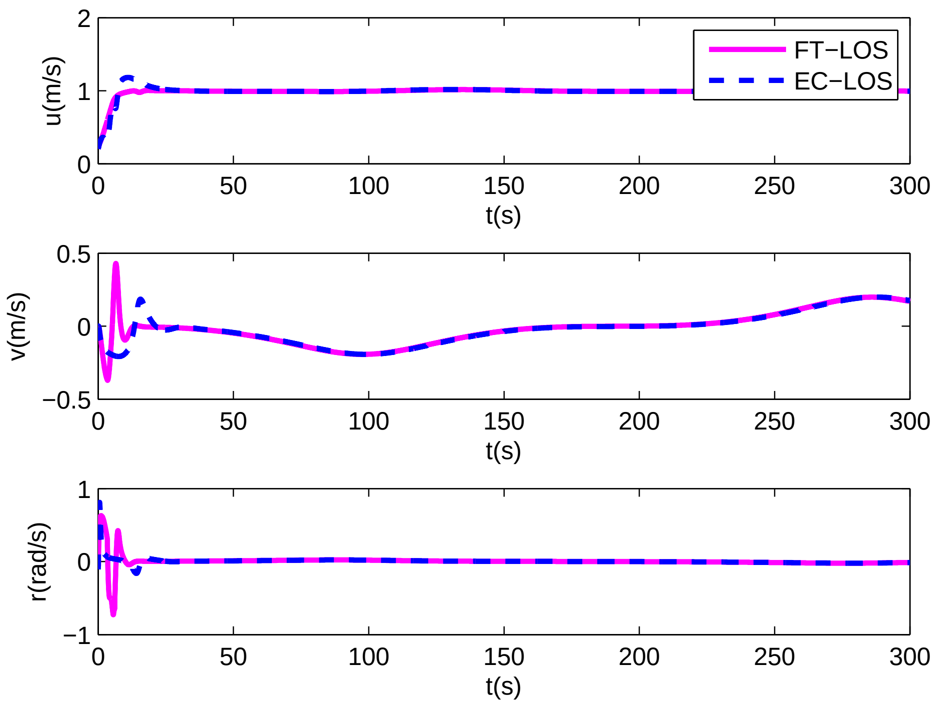

Figure 5. The surge velocity, sway velocity and yaw angle velocity of the underactuated MSV.

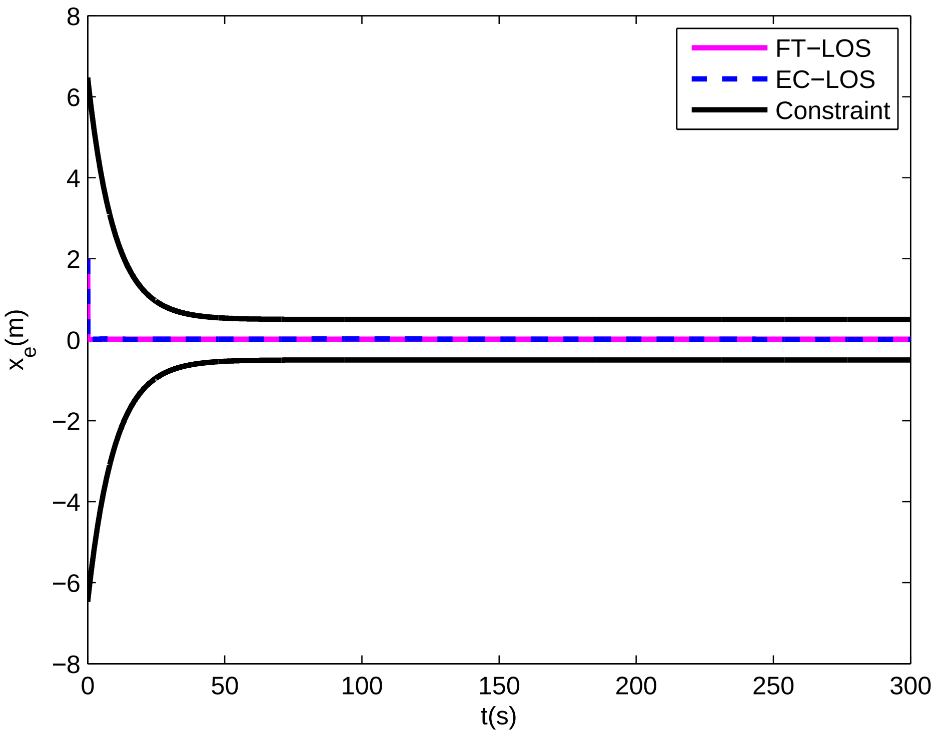

Figure 6. Along-track error of the underactuated MSV by different guidance laws.

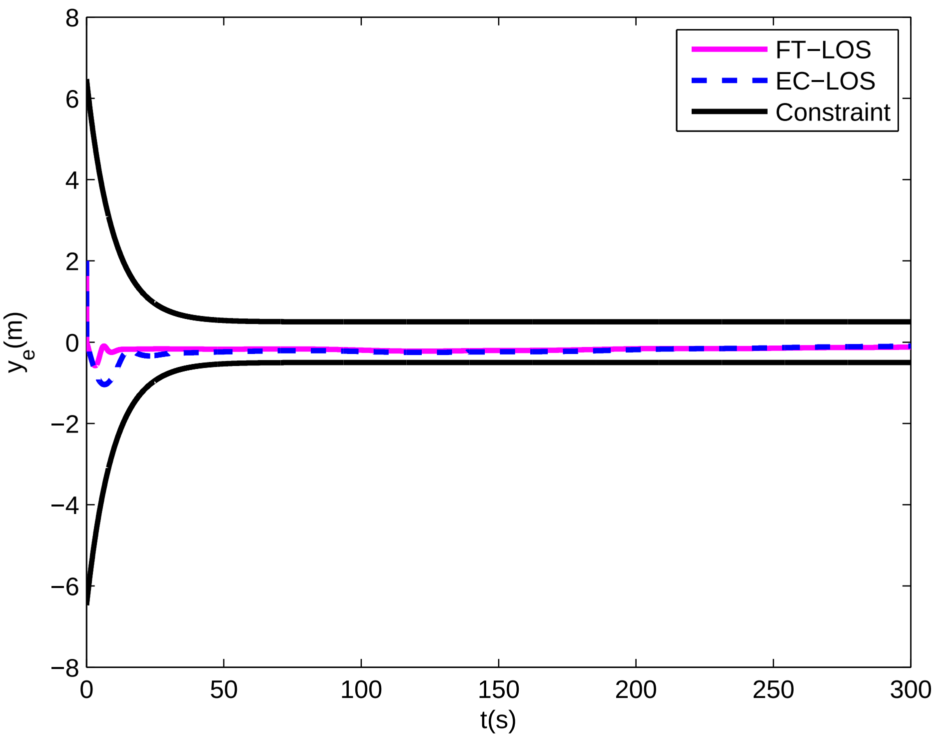

Figure 7. Cross-track error of the underactuated MSV by different guidance laws.

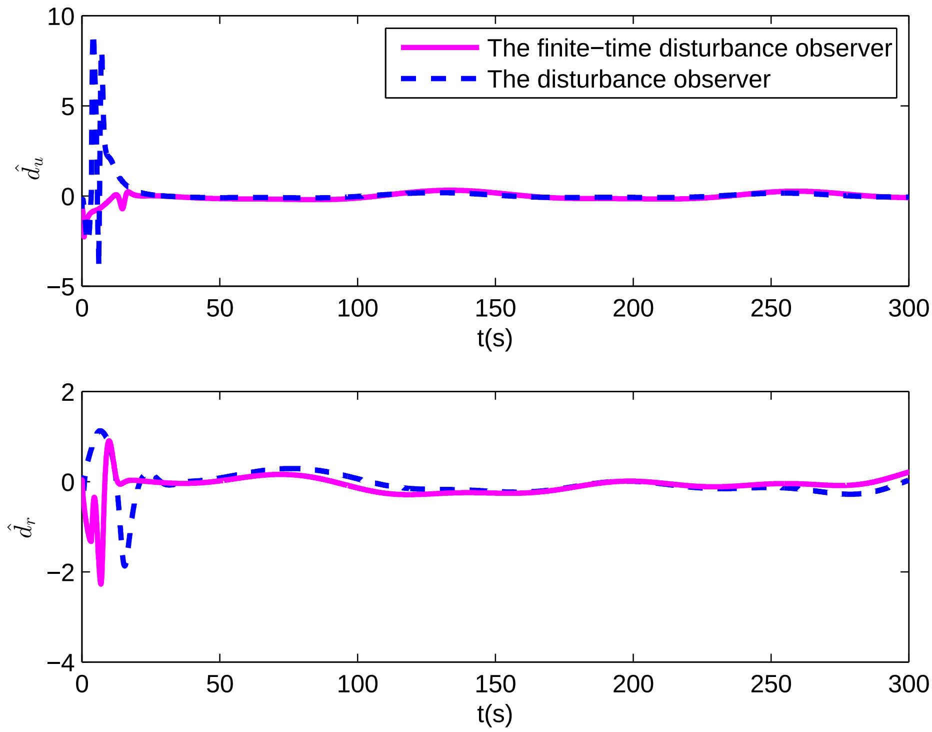

Figure 8. The estimation errors by different disturbance observers.

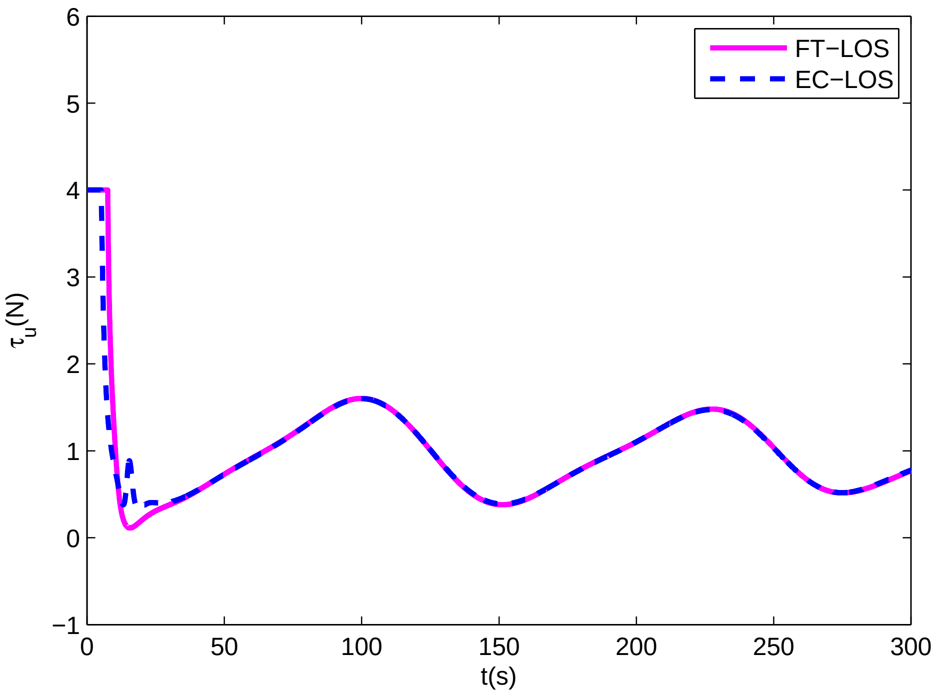

Figure 9. The surge force τ_u under the input saturation.

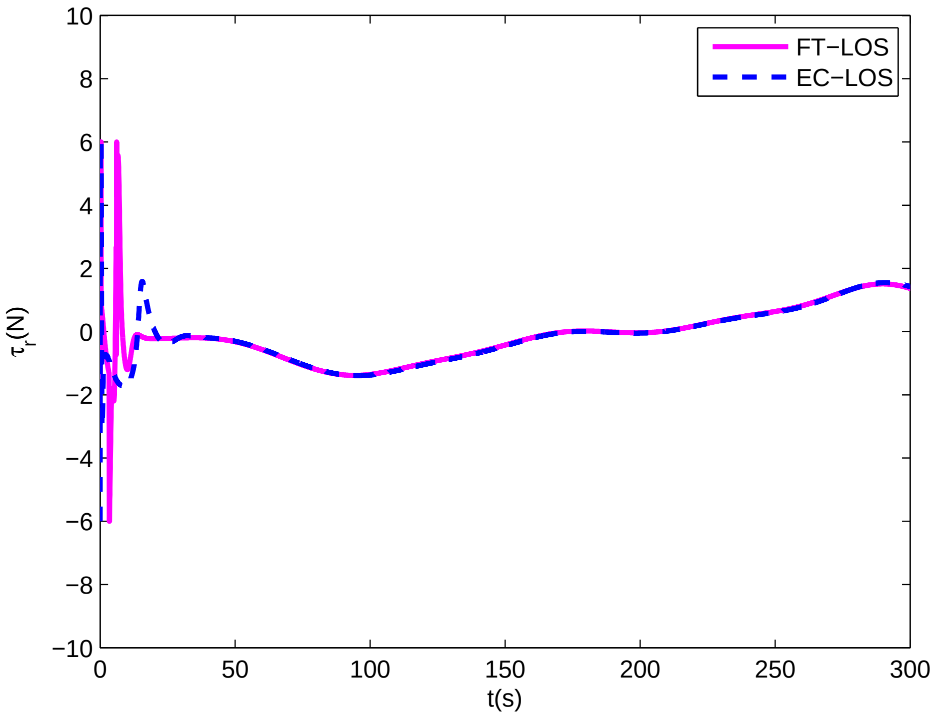

Figure 10. The yaw moment τ_r under the input saturation.

6. Conclusions

In this paper, a finite-time path following control algorithm has been presented for the underactuated MSV with external disturbances, model parametric uncertainties, position constraint and input saturation. Different from the existing literature, position error constraints, input saturation and finite convergence time are simultaneously considered in the control design. The FT-LOS guidance law is designed to obtain the desired yaw angle and simultaneously constrain the position error of the underactuated MSV. The finite-time constraint controllers are designed to achieve tracking control in finite time. Then, the finite-time disturbance observers are proposed to estimate the compound disturbance including the external disturbances and model parametric uncertainties. Additionally, the finite-time input saturation compensators are designed to avoid the actuator saturation and satisfy the requirement of finite-time convergence. The stability analysis shows that the proposed finite-time control algorithm can strictly guarantee the constraint requirement of the position, and all error signals of the whole control system can converge into a small neighborhood around zero in finite time. Eventually, comparative simulation results illustrate the effectiveness and superiority of the proposed finite-time control algorithm. In future work, we will consider the unknown sideslip angle and time delays in the underactuated MSV.

Author Contributions: Methodology, L.W.; Software, L.W.; Supervision, M.F.; Writing—original draft, L.W.; Writing—review and editing, L.W. All authors have read and agreed to the published version of the manuscript.

Funding: This work was supported by the National Nature Science Foundation of China under Grant 51879049.

Conflicts of Interest: The authors declare no conflict of interest.

Abbreviations

The following abbreviations are used in this manuscript:

MSV	Marine surface vessel
LOS	Line-of-sight
BLF	Barrier Lyapunov function
FT-LOS	Finite-time line-of-sight
PLOS	Proportional line-of-sight
ILOS	Integral line-of-sight
EC-LOS	Error-constrained line-of-sight

References

1. Børhaug, E.; Pavlov, A.; Pettersen, K.Y. Straight line path following for formations of underactuated underwater vehicles. In Proceedings of the 46th IEEE Conference on Decision and Control, New Orleans, LA, USA, 12–14 December 2007; pp. 2905–2912.
2. Breivik, M.; Fossen, T.I. *Guidance Laws for Autonomous Underwater Vehicles*; In Tech: Vienna, Austria, 2009; pp. 51–76.
3. Breivik, M.; Hovstein, V.E.; Fossen, T.I. Straight-line target tracking for unmanned surface vehicles. *Model. Ident. Control* **2009**, *29*, 131–149. [CrossRef]
4. Muresan, M.P.; Giosan, I.; Nedevschi, S. Stabilization and validation of 3D object position using multimodal sensor fusion and semantic segmentation. *Sensors* **2020**, *20*, 1110. [CrossRef] [PubMed]
5. Fossen, T.I. *Handbook of Marine Craft Hydrodynamics and Motion Control*; Wiley: New York, NY, USA, 2011.
6. Breivik, M.; Fossen, T.I. Path following for marine surface vessels. In Proceedings of the Oceans MTS/IEEE Technology-Ocean, Kobe, Japan, 9–12 November 2004; Volume 4, pp. 2282–2289.
7. Børhaug, E.; Pavlov, A.; Panteley, E.; Pettersen, K.Y. Straight line path following for formations of underactuated marine surface vessels. *IEEE Trans. Contr. Syst. Technol.* **2011**, *19*, 493–506. [CrossRef]
8. Balch, T.; Arkin, R.C. Behavior-based formation control for multirobot teams. *IEEE Trans. Robot. Autom.* **1998**, *14*, 926–939. [CrossRef]
9. Fossen, T.I. *Marine Control System: Guidance, Navigation and Control of Ship*; Rigs and Underwater Vehicles: Trondheim, Norway, 2002.
10. Fossen, T.I.; Breivik, M.; Skjetne, R. Line-of-sight path following of underactuated marine craft. *IFAC Proc. (MCMC)* **2003**, *36*, 211–216. [CrossRef]
11. Børhaug, E.; Pavlov, A.; Pettersen, K.Y. Integral LOS control for path following of underactuated marine surface vessels in the presence of constant ocean currents. In Proceedings of the 47th IEEE Conference on Decision and Control, Caucun, Mexico, 9–11 December 2008; pp. 4984–4991.
12. Caharija, W.; Pettersen, K.Y.; Bibuli, M.; Calado, P.; Zereik, E.; Braga, J.; Bruzzone, G. Integral line-of-sight guidance and control of underactuated marine vehicles: Theory, simulations, and experiments. *IEEE Trans. Control Syst. Technol.* **2016**, *24*, 1623–1642. [CrossRef]
13. Fu, M.; Wang, T.; Wang, C. Barrier Lyapunov function-based adaptive control of an uncertain hovercraft with position and velocity constraints. *Math. Probl. Eng.* **2019**, *2019*, 1940784. [CrossRef]
14. Zheng, Z.; Sun, L.; Xie, L. Error-constrained LOS path following of a surface vessel with actuator saturation and faults. *IEEE Trans. Syst. Man Cybern. Syst.* **2018**, *48*, 1794–1805. [CrossRef]
15. Zheng, Z.; Huang, Y.; Xie, L; Zhu, B. Adaptive trajectory tracking control of a fully actuated surface vessel with asymmetrically constrained input and output. *IEEE Trans. Control Syst. Technol.* **2018**, *26*, 1851–1859. [CrossRef]
16. Zheng, Z.; Feroskhan, M. Path following of a surface vessel with prescribed performance in the presence of input saturation and external disturbances. *IEEE/ASME Trans. Mechatron.* **2017**, *22*, 2564–2575. [CrossRef]
17. Nie, J.; Lin, X. Robust nonlinear path following control of underactuated MSV with time-varying sideslip compensation in the presence of actuator saturation and error constraint. *IEEE Access* **2018**, *36*, 71906–71917. [CrossRef]
18. Wang, Y.; Tong, H.; Wang, C. High-gain observer-based line-of-sight guidance for adaptive neural path following control of underactuated marine surface vessels. *IEEE Access* **2019**, *7*, 26088–26101. [CrossRef]

19. Wang, C.; Wu, Y.; Yu, J. Barrier Lyapunov functions-based dynamic surface control for pure-feedback systems with full state constraints. *IET Control Theory Appl.* **2017**, *11*, 524–530. [CrossRef]
20. Liu, S.Y.; Liu, Y.C.; Wang, N. Nonlinear disturbance observer-based backstepping finite-time sliding mode tracking control of underwater vehicles with system uncertainties and external disturbances. *Nonlinear Dyn.* **2017**, *88*, 465–476. [CrossRef]
21. Wang, N.; Sun, Z.; Yin, J.; Su, S.F.; Sharma, S. Finite-time observer based guidance and control of underactuated surface vehicles with unknown sideslip angles and disturbances. *IEEE Access* **2018**, *6*, 14059–14070. [CrossRef]
22. Nie, J.; Lin, X. FAILOS guidance law based adaptive fuzzy finite-time path following control for underactuated MSV. *Ocean Eng.* **2019**, *195*, 106726. [CrossRef]
23. Tee, K.P.; Ge, S.S.; Tay, E.H. Barrier Lyapunov functions for the control of output-constrained nonlinear systems. *Automatica* **2009**, *45*, 918–927. [CrossRef]
24. Bhat, S.P. Finite-time stability of continuous autonomous systems. *SIAM J. Control Optim.* **2000**, *38*, 751–766. [CrossRef]
25. Xia, J.; Zhang, J.; Sun, W.; Zhang, B.; Wang, Z. Finite-time adaptive fuzzy control for nonlinear systems with full state constraints. *IEEE Trans. Syst. Man Cybern. Syst.* **2019**, *49*, 1541–1548. [CrossRef]
26. Wang, L.; Xiao, F. Finite-time consensus problems for networks of dynamic agents. *IEEE Trans. Autom. Control* **2010**, *55*, 950–955. [CrossRef]
27. Fossen, T.I.; Pettersen, K.Y.; Galeazzi, R. Line-Of-Sight path following for dubins paths with adaptive sideslip compensation of drift forces. *IEEE Trans. Control Syst. Technol.* **2015**, *23*, 820–827. [CrossRef]